International Journal of Technical Research and Applications e-ISSN: 2320-8163,
www.ijtra.com Volume 4, Issue 1 (January-February 2016), PP. 234-240

The Bayesian Framework for Single Image Dehazing in desert area images considering Noise

Tabrej Khan
Faculty of Science
Institute of Computer Science & Information Technology
Bundelkhand University, Jhansi,
UP,India

***Abstract*— The Bayesian structure has considered noise and haze with the aim of meeting the dehazing algorithms. The research paper below contains a brief introduction of the existing desert image dehazing algorithms. A literature review containing the development and aim of the Bayesian framework is also outlined in the research paper. The research objective is outlined, with the three methodologies used in the research discussed in detail. It is here that different formulas associated with the proposed algorithm have been discussed. Later is the evaluation of the proposed desert image dehazing algorithm, with the most efficient approach being identified? The paper ends with a short conclusion, summarizing all the main ideas that have been discussed in the entire research paper.**

I. INTRODUCTION

The existing single desert area image dehazing algorithms only have the ability satisfy the demand for dehazing efficiency, leaving behind the need for denoising. Single image dehazing is an underlying issue and also an essential topic in the area of image processing which is aimed at two aspects. One of the elements is to create a visually attractive image that is appropriate for mortal pictorial perception. The other element for the single image dehazing is to advance the interpretability of pictures for preprocessing errands and computer image (Lengyel et al. 2000).

II. REVIEW OF LITERATURE

The aim of the Bayesian structure for single image dehazing considering noise was to solve the problem that the existing dehazing algorithms fail to satisfy. A good single image dehazing algorithm ought to remove noise and haze simultaneously and efficiently (Kush, & Kansal, 2015). For the exiting dehazing algorithms, there are two methods. One of the ways is grounded on image development techniques and purposes at directly improving the image graphic effect such as the Retinex and histogram equalization (Zhu et al. 2015). This method is fast and straightforward. However, it has a high relevance and cannot adjust all the image features to a proper collection. Also, it fails to improve the image features by the human visual system. The other method in the existing dehazing algorithm has its basis on the technique of image restoration. This method has a strong assumption atmospheric transmission, making it possible to solve the problems arising from atmospheric scattering that possesses ill-posedness, such as the Tan optimization that is founded on the Markov random field and the Fattal estimation which is established by the independent component analysis. However, this method is over-reliant on the environmental luminance model, not to mention its vulnerability to the external environment (Ancuti, 2013).

After analysis of the current dehazing founded on image restoration, it is evident that most of the algorithms are only focused on improving the luminance and contrast of the degraded image. They fail to cater for noise, which has become a significant and global issue in dehazing. In 2012, instantaneous dehazing and denoising founded on the combined two-sided filter were realized and were found to be causing excessive enhancement. It was in this year that two other methods were proposed for the removal of fog and noise in a particular image. On the method involved denoising the image before dehazing while the other entailed a collaborative regression method. The strength of these two methods is that they have a right performance when the level of noise is known. However, the two methods have a weakness in that latent errors are likely to be amplified from denoising or over denoising where the levels of noise are not explicitly known. In 2013, a haze image model was presented, considering both noise and sensor blur. The single image dehazing algorithm was categorized as a technique for improving images in the previous times. It was modeled by Middleton in 1952 as an image transformation technique and was later developed into a mature model by McCartney, where it was centered on Rayleigh scattering. This model was cast-off to define the creation of the besmirched image in 1976.

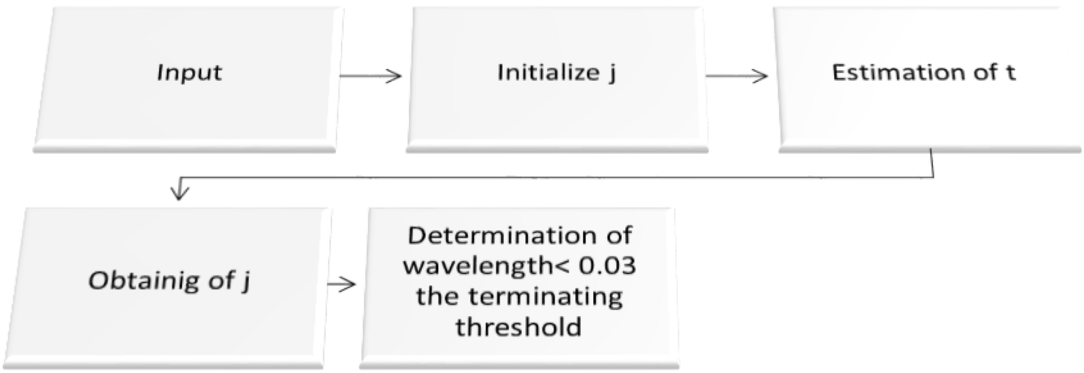

Fig1. The iterative method with view founded on the rule of minimum noise level.

III. Research objectives

This research paper will be aimed at proposing the Bayesian structure which would prevent vibrant range density in the He's compression. For this proposed structure, the accuracy of the input desert area image is ensured through the simultaneous removal of haze and noise.

IV. Methodology

This paper will have a momentary overview of the McCartney's atmospheric scattering ideal and later make proposals for enhanced atmospheric scattering model founded on its flaws. It is popular that an image that is acknowledged by a beam from the scene themes is frequently captivated and dispersed through an intricate medium. When it comes to computer image and distinctive optics, the McCartney's atmospheric smattering plays a significant part in the ruin of the image (Wang et al. 2015). Below is the equation (1) for the McCartney's atmospheric scattering model:

$$I(a, c) = t(a, c)\, J(a, c) + (1 - t(a, c))\, A$$

In the above formula, I (a, c) represents the detected besmirched image, while J (a, c) represents the section radiance which is a representation of the initial image appearance. A is the universal atmospheric light that is most identified as the mean of upper 0.6% brightest megapixels in the haze image. t (a, c) is the representation of the atmospheric transmission plot. The problem with this equation arises in the estimation of the hidden image J (a, c) from I (a, c) where t (a, c) is provided, thus making it an abnormal equation (Wang et al. 2015).

Since the noise and sensor from the environment are considered to be significant degradation factors and are not recognized in the McCartney's atmospheric scattering model, then the below equation (2) would be proposed as an enhanced atmospheric scattering model:

$$I(a, c) = t(a, c)\, J(a, c) + (1 - t(a, c))\, A + n(a, c)$$

In the above equation, n (a, c) represents a zero mean Gaussian noise while it originates from the sensor and the environment. In this proposed method, there are two types of approaches, where the first approach would involve a step by step dehazing and denoising. The second approach would be a simultaneous denoising and dehazing (Lee et al. 2016). The former involves denoising before haze removal and haze removal before denoising. Haze removal before haze removal can lead to information loss on the image details (Bodart et al, 2015). The equation (3) for dehazing before removing eliminating noise is represented below:

$$J(a, c) = A + (I(a,c) - A)/(t(a,c)) - (n(a,c)dc)/(t(a,c))$$

In the above equation, t (a, c) represents a value in the range of 0 as well as 1, where it differs in reverse with the light concentration. This equivalence infers that failure to remove the noise before dehazing leads to the amplification of the noise. This case is likely to be experienced in the last hazy areas where t (a, c) is a representation adjacent to 0, with noise influence dominating the results

The proposed approach in this research will be based on a combination of the following, to achieve a balance between denoising and dehazing:

Best of the Bayesian framework

Iterative algorithm with feedback

Statistical preceding and objective hypothesis of the degraded image

Below is our approaches' establishment that is based on the Bayesian framework:

After rearranging the equation 2, the following expression (4) was arrived at:

I (a, c) – A= (J (a, c) - A) t (a, c) + n (a, c)a_(c^2)

For our approach to keep nonnegative, a reversal is done to produce an expression (5) as indicated below:

I_(A^((a,c)=)) J_(A^((a,c)t(a,c)-n(a,c))), where I_(A^((a,c)=A-I(a,c),)) J_(A^((a,c)=A-J(a,c)))

We obtained the probability density function through three methods, where the first method involved obtaining preceding probability density task based on the approximation of the noise level (Makarau et al. 2014). Here, we assumed that the noise and the signal are correlated, and the adjustment on the direction (u) can be expressed as follows:

〖V(u〗 ^T I_(A^))= 〖V(u〗 ^T J_(A^) t)+σ 〖^2〗, where V (a) is a representation of the variance dataset a; σ represents the standard deviation of the Gaussian noise. Our definition for the least variance direction is u_(〖min〗 ^as)

u_(〖min〗 ^as)=arg (_1 ^min)V(u^T I_(A^))= arg(_u ^min) V 〖(u〗 ^T J_(A^) t)

Our second method involved finding of J_(A^('s))chance concentration function founded on dissemination of chromaticity gradient histogram (Shen et al. 2015). We randomly analyzed some designated haze photos with their photos without haze. After the analysis, we found out that the scattering of chromaticity gradient histogram of the photos with haze is similar to their haze-free images that represent the influence of the exponential power of distribution Kush & Kansal, 2015). Consider the two images below:

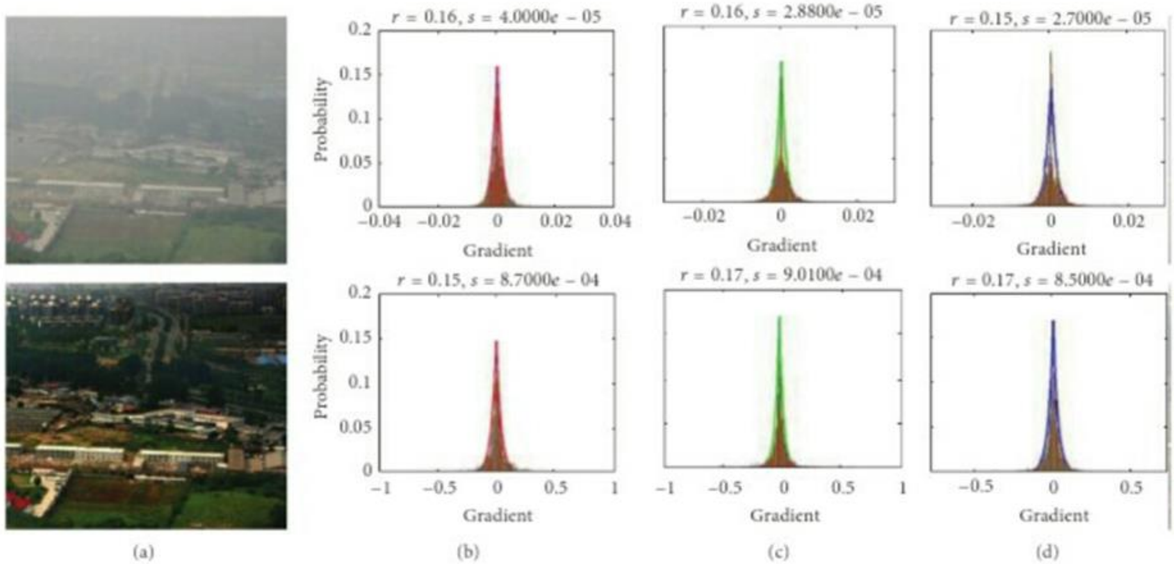

Fig.2 Chromaticity gradient histogram distribution Upper: the haze photo. Bottommost: the haze-free image (a) Haze photo and its haze-free photo, (b) Chromaticity gradient histogram dispersal of red light constituent, (c) Chromaticity gradient histogram dissemination of green light constituent, (d) Chromaticity gradient histogram dissemination of blue light element.

The first image is a representation of a haze image. The second one represents a haze-free image. The two images have a horizontal and vertical gradient with the following:

- The haze photo with its haze-free photo
- Dissemination of chromaticity gradient histogram of red light constituent
- Dissemination of chromaticity gradient histogram of green light constituent
- Dissemination of chromaticity gradient histogram of blue light constituent

The two above images are exponentially distributed, with the only difference occurring in their rate and normalization parameters. The second image exhibits a Mean Squared Error (MSE) amid the dissemination of chromaticity gradient histogram and their exponential power dissemination of the hazed images that we sampled together with their haze-free images (Nan et al. 2014). We found from the experiment that the exponential power distribution is reliable for fitting since their MSE are still at the low level.

Our third method involved attaining of the t's chance density function founded on the sensitivity of green wavelength. Since the human optical coordination has a precise reaction sensitivity to the insignificant intermission of light wavelength, we were able to identify that there existed both photonic and scotopic responses (Toet et al, 2016). We also found out that the two answers have a concentrated sensitivity from green-blue wavelength for red and blue view. However, we also identified that the scotopic vision has a complex sensitivity to glowing efficacy than the photopic vision (Liu, et al. 2015).

V. RESULTS

After conducting our experiment, we were able to gather the following results as indicated by the photos:

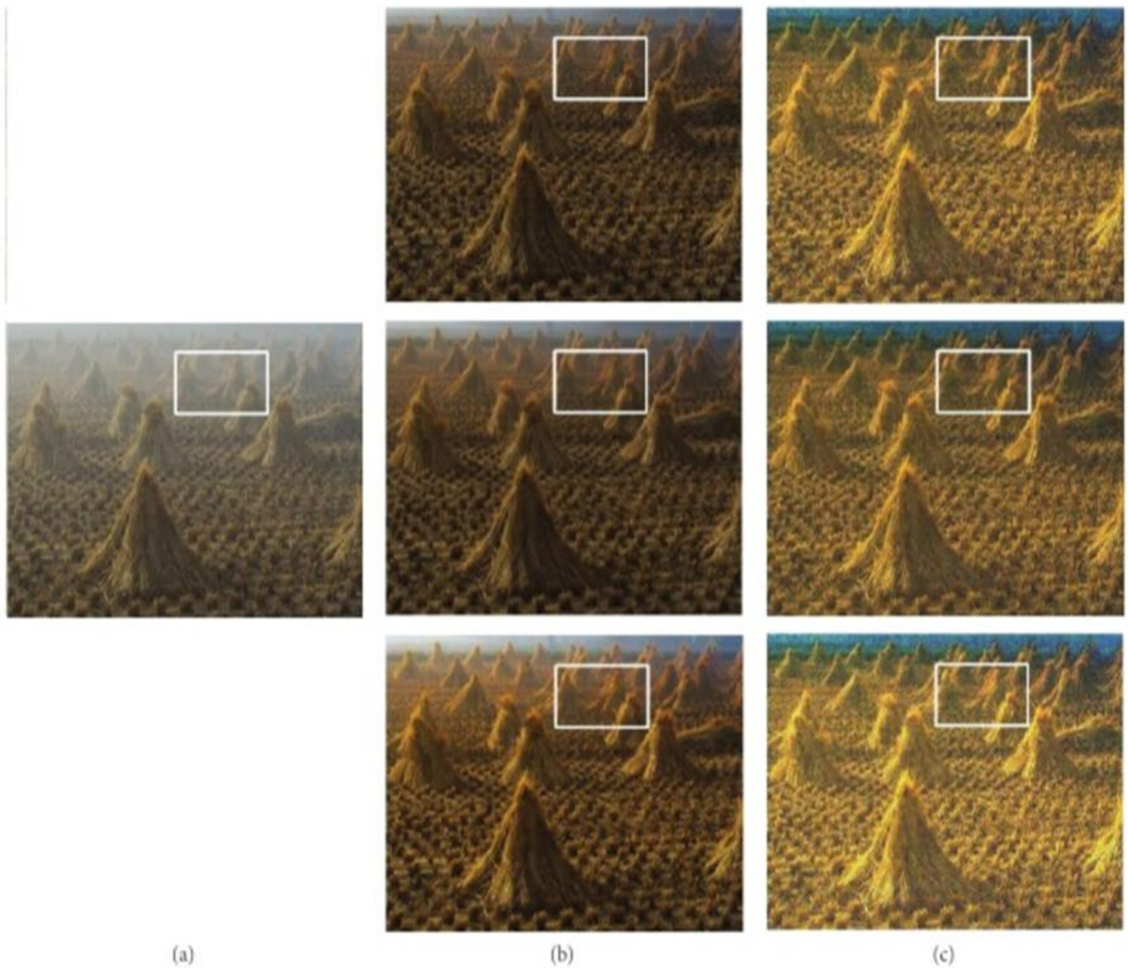

Fig3. Natural images (Desert):

Input

(b) The dissimilarity tests: from highest to lowest; He's outcome, He-BM3D's outcome and Lan's outcome and

(c) Bayesian framework outcome: From highest to lowest; first repetition, second repetition and third repetition.

(a)

(b)

(c)

(a)

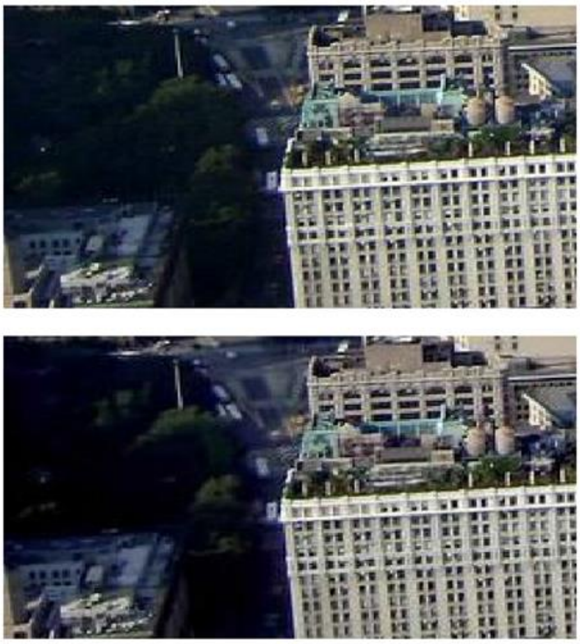

(b)

(c)

In the figures.
Input
He's result and Lan's result respectively
He-BM3D and our result respectively.

The comparative figures of before and after enlargement indicate the deep depth photo with loads of specifics and multifaceted noise. He's process might intensify the noise and misplace texture info. Denoising by BM3D will result to detail loss. Lan's algorithm too cannot reinstate section and facts in the great depth area efficiently. Our outcome, in dissimilarity, could show more vivid restored image with high contrast and obtain nearly the similar haze-free photo as He's outcome. In specific, the projected procedure accomplishes wider active range density in dark areas.

The figure below shows that our outcome accomplishes nearly the same noise level like the Lan's outcome and becomes approximately the same result as He's outcome in haze removal. Therefore, we see that the individual evaluation approves the objective one.

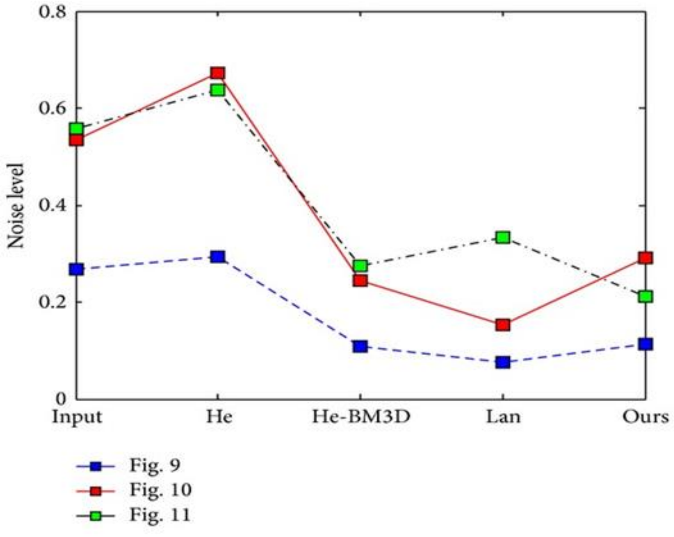

(a)

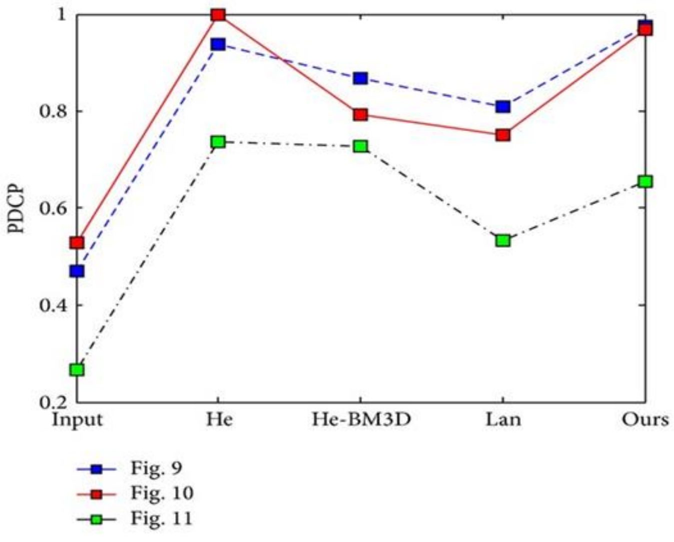

(b)

Fig. Proposed algorithm noise level and expected outcome compared to Lan's and He's outcome in haze removal

VI. Discussion

The proposed algorithm attains a wider vibrant range compression within regions that are dark and has a strong ability for noise resistance. Hence, the results for our research as explained above indicate that our proposed algorithm had the capability of attaining noise levels that are close to the He's and Lan's algorithms. For the dehazing effect, our proposed algorithm had almost a similar effect with the He's algorithm. However, the Lan's algorithm has no ability for restoring scene, together with details within a large depth area in an efficient manner, which makes our proposed method to be more superior to the latter. Due to the achievement of positive effects in denoising and dehazing, the capacity of our proposed approach in scene restoration and protection of detail is well demonstrated.

EVALUATION

To validate the results that we gathered from our research, we established four methods indicated below:

- Mock images with noise and haze to examine performance
- Close distance images for performance testing
- Close depth images with noise for performance testing
- Deep depth images with their local enlargements for performance testing

After examination of the above four methods, we found that the use of synthetic images with noise and haze to test performance was capable of removing noise and fog more efficiently than the other three. Our approach indicates that it is capable of denoising and dehazing, which makes it suitable for scene restoration and protection of detail (Sun et al. 2015).

CONCLUSION

The research paper above presented the single image dehazing approach, making an allowance for noise based on the Bayesian framework. The paper focused on enhanced atmospheric scattering model which was based on sound and haze. The paper also focused more on the efficiency by selecting the transmission map to arrive at the scene radiance. Though the methodologies applied in the research paper, it can be concluded that the proposed approach is useful, particularly in the challenging of scenes with both noise and haze.

REFERENCES

Zhu, Q., Mai, J., & Shao, L. (2015). A fast single image haze removal algorithm using color attenuation prior. IEEE Transactions on Image Processing, 24(11), 3522-3533.

Ancuti, C. O., & Ancuti, C. (2013). Single image dehazing by multi-scale fusion. IEEE Transactions on Image Processing, 22(8), 3271-3282.

Wang, J. B., He, N., Zhang, L. L., & Lu, K. (2015). Single image dehazing with a physical model and dark channel prior. Neurocomputing, 149, 718-728.

Wang, J., He, N., & Lu, K. (2015, August). A new single image dehazing method with MSRCR algorithm. In Proceedings of the 7th International Conference on Internet Multimedia Computing and Service (p. 19). ACM.

Lee, S., Yun, S., Nam, J. H., Won, C. S., & Jung, S. W. (2016). A review on dark channel prior based image dehazing algorithms. EURASIP Journal on Image and Video Processing, 2016(1), 4.

Nan, D., Bi, D. Y., Liu, C., Ma, S. P., & He, L. Y. (2014). A Bayesian framework for single image dehazing considering noise. The Scientific World Journal, 2014.

Makarau, A., Richter, R., Muller, R., & Reinartz, P. (2014). Haze detection and removal in remotely sensed multispectral imagery. IEEE Transactions on Geoscience and Remote Sensing, 52(9), 5895-5905.

Kush, N., & Kansal, A. G. (2015). Performance evolution of improvement in change detection techniques based on edge enhanced images (Doctoral dissertation).

Toet, A., Hogervorst, M. A., & Pinkus, A. R. (2016). The TRICLOBS Dynamic Multi-Band Image Data Set for the Development and Evaluation of Image Fusion Methods. PloS one, 11(12), e0165016.

Sun, W., Li, D., Jia, W., Li, P., Zhao, C., & Chen, X. (2015, September). Small Moving Object Tracking in Dynamic Video. In Intelligent Information Hiding and Multimedia Signal Processing (IIH-MSP), 2015 International Conference on (pp. 239-242). IEEE.

Shen, Y., Wang, Y., Lv, H., & Qian, J. (2015). Removal of Thin Clouds in Landsat-8 OLI Data with Independent Component Analysis. Remote Sensing, 7(9), 11481-11500.

Lengyel, J. E., & Snyder, J. (2000). U.S. Patent No. 6,016,150. Washington, DC: U.S. Patent and Trademark Office.

Bodart, C., Eva, H., Beuchle, R., Raši, R., Simonetti, D., Stibig, H. J., ... & Achard, F. (2011). Pre-processing of a sample of multi-scene and multi-date Landsat imagery used to monitor forest cover changes over the tropics. ISPRS Journal of Photogrammetry and Remote Sensing, 66(5), 555-563.

Liu, L., Li, B., Yang, S., Guo, M., Yan, M., Luo, T., ... & Gao, S. (2015, October). Polarization difference imaging of objects in smoke environment. In AOPC 2015: Optical Design and Manufacturing Technologies (Vol. 9676, p. 96760J). International Society for Optics and Photonics. 1989.